NIH Public Access
Author Manuscript
Biochem J. Author manuscript; available in PMC 2014 March 24.

Published in final edited form as:
Biochem J. 2011 March 15; 434(3): 415–426. doi:10.1042/BJ20101437.

Receptor-dependent compartmentalization of PPIP5K1, a kinase with a cryptic polyphosphoinositide binding domain

Nikhil A. Gokhale[1], **Angelika Zaremba**[1], and **Stephen B. Shears**[2]
Inositol Signaling Group, Laboratory of Signal Transduction, National Institute of Environmental Health Sciences, NIH, DHHS, Research Triangle Park, PO Box 12233, NC 27709, U.S.A

Abstract

The inositol pyrophosphates are multifunctional signalling molecules. One of the families of enzymes that synthesize the inositol pyrophosphates are the Vip1/PPIP5Ks (PP-InsP_5 kinases). The kinase domains in Vip1/PPIP5Ks have been mapped to their N-terminus. Each of these proteins also possess a phosphatase-like domain of unknown significance. In the present study, we show that this phosphatase-like domain is not catalytically active. Instead, by using SPR (surface plasmon resonance) to study protein binding to immobilized lipid vesicles, we show that this domain is specialized for binding PtdIns(3,4,5)P_3 (PPIP5K1 K_d = 96 nM; PPIP5K2 K_d = 705 nM). Both PtdIns(3,4)P_2 and PtdIns(4,5)P_2 are significantly weaker ligands, and no significant binding of PtdIns(3,5)P_2 was detected. We confirm the functional importance of this domain in inositol lipid binding by site-directed mutagenesis. We present evidence that the PtdIns(3,4,5)P_3-binding domain is an unusual hybrid, in which a partial PH (pleckstrin homology) consensus sequence is spliced into the phosphatase-like domain. Agonist-dependent activation of the PtdIns 3-kinase pathway in NIH 3T3 cells drives translocation of PPIP5K1 from the cytosol to the plasma membrane. We have therefore demonstrated receptor-regulated compartmentalization of inositol pyrophosphate synthesis in mammalian cells.

Keywords

cell-signalling; compartmentalization; diphosphoinositol polyphosphates; inositol pyrophosphates

INTRODUCTION

The phospholipase C-initiated synthesis of the inositol pyrophosphates (e.g. PP-InsP_5 and [PP]$_2$-InsP_4) is proposed to be a primordial signalling pathway that predates the evolution of the Ins(1,4,5)P_3-activated Ca^{2+}-mobilization cascade [1]. These inositol pyrophosphates have been proposed to regulate a variety of cellular activities (for reviews see [2–4]), including apoptosis, vesicle trafficking, cytoskeletal dynamics, exocytosis, telomere maintenance and adaptations to environmental stress. Eukaryotic cells typically contain one isomer of [PP]$_2$-InsP_4 (with diphosphates at the 1/3 and 5 positions [5]) which is synthesized from either of two isomers of PP-InsP_5 (the 1/3 and 5 isomers). Two families of proteins collaborate to synthesize these molecules. Three members of the IP6K (InsP_6 kinase) family [6] convert InsP_6 to 5-PP-InsP_5 [7] and these enzymes can also synthesize 1/3,5-[PP]$_2$-InsP_4

© The Authors Journal compilation

[2]To whom correspondence should be addressed (Shears@niehs.nih.gov).
[1]These two authors contributed equally to this study.

AUTHOR CONTRIBUTION
All three of the authors designed and performed experiments, and contributed to writing the manuscript.

NIH-PA Author Manuscript
NIH-PA Author Manuscript
NIH-PA Author Manuscript

NIH-PA Author Manuscript

NIH-PA Author Manuscript

NIH-PA Author Manuscript

from 1/3-PP-InsP_5 [5]. There are also two PPIP5K (PP-InsP_5 kinase) enzymes [8,9] (Vip1 in yeasts [10]) that add a 1/3-diphosphate to both InsP_6 and 5-PP-InsP_5 [5].

Even the most abundant of the inositol pyrophosphates (5-PP-InsP_5 [11]) is typically present in cells at 20-fold lower levels than those of InsP_6 [3,4]. This difference in polyphosphate concentrations has raised some questions concerning proposed mechanisms of action of the inositol pyrophosphates, particularly as they are so similar in structure to InsP_6 [3,4]. For example, a receptor for one particular inositol pyrophosphate would have to be remarkably specific in order to prevent competition or inhibition from InsP_6, or indeed from any of the other inositol pyrophosphates; it is challenging to anticipate at a molecular level how the requisite specificity could be achieved [3]. To illustrate this point, it is notable that even the IP6K and Vip1/PPIP5K kinases recognize both InsP_6 and PP-InsP_5 (see above). Even when it has been shown that InsP_6 neither mimics nor inhibits the binding of an inositol pyrophosphate (i.e. 1/3-PP-InsP_5) to its receptor (a yeast cyclin–cyclin kinase complex [12,13]) there can sometimes be concern over biological relevance. In the latter case, the affinity for 1/3-PP-InsP_5 appears too low to permit it, at ‘global’ physiologically relevant levels, to bind effectively to its target [4]. These are persistent questions in this field.

An alternative and less traditional mechanism of action of inositol pyrophosphates has come from studies *in vitro* that have described a novel mechanism of post-translation modification by the inositol pyrophosphates: the kinase-independent transfer to appropriate target proteins of their ‘high-energy’ diphosphate groups [14–16]. The proliferation of the number of apparent protein targets [14,16] could help explain why these pyrophosphates appear to regulate so many diverse cellular processes. However, as InsP_6 strongly inhibits transphosphorylation by inositol pyrophosphates [15], this mechanism of action still faces the difficulty that InsP_6 is relatively abundant [4]. There is also the issue that the entire family of inositol pyrophosphates has the ability to transphosphorylate proteins [14]. That observation raises the question of why are there multiple members of the inositol pyrophosphate family that each perform an identical function? Furthermore, in a scenario in which inositol pyrophosphates are, like all soluble signals, free to diffuse quickly through the cell, how could a single member of this family of molecules be recruited to perform one specific signalling task by a particular extracellular stimulus?

All of these difficulties in understanding the molecular basis for specificity in signalling by inositol pyrophosphates have a potential solution in the proposal that there might be spatially restricted synthesis of an inositol pyrophosphate [3]. For example, locally elevated levels of a particular inositol pyrophosphate would make InsP_6 a less effective competitor, both in the context of mechanisms that involve receptor binding or transphosphorylation. Co-localization of the synthesis of one particular inositol pyrophosphate with a protein target could also facilitate specificity of signalling.

This idea that any ‘freely diffusible’ intracellular signal might be compartmentalized within a single cell was for a long time a heretical concept. Now the idea is mainstream, and the paradigm shift owes much to the characterization of spatial localization of cAMP signalling [17]. In this example, the enzymes that synthesize cAMP are spatially separated from the enzymes that hydrolyse cAMP, thereby generating an intracellular concentration gradient for this signal. By the same principle, an intracellular inositol phosphate concentration gradient is possible [18]. Certain inositol phosphate kinases possess nuclear retention signals [19,20]. It can therefore be anticipated that there might be some inositol phosphate concentration gradients across the nuclear membrane. However, the spatial organization of cytoplasmic signalling by inositol phosphates is less well understood. Arguably the most striking observation to date is the Ca^{2+}-dependent exodus of the type A Ins(1,4,5)P_3 3-kinase out of the spines of pyramidal neurons [21]. This change in the localization of Ins(1,4,5)P_3

NIH-PA Author Manuscript

NIH-PA Author Manuscript

NIH-PA Author Manuscript

metabolism is believed to contribute to setting the temporal and spatial dynamics of neuronal Ca^{2+} signalling [21]. Among the other components of the cytoplasmic inositol phosphate cascade, evidence of enzyme compartmentalization is patchy and there is little information on molecular mechanisms or biological significance. For example, it is unknown how and why the Ins(1,3,4)P_3 5/6-kinase is sometimes restricted to the plasma membrane [22], or why the Ins(1,3,4,5,6)P_5 2-kinase is concentrated in cytoplasmic stress granules [19]. Nevertheless, in the light of recent evidence that Ins(1,3,4,5,6)P_5 and $InsP_6$ may each be distributed between two or more metabolically-distinct pools, there is growing interest in the general significance to cell signalling of compartmentalization of inositol phosphates [23].

In the present study we demonstrate that cytoplasmic compartmentalization of inositol pyrophosphate synthesis is not only possible, but it is also receptor-regulated. We show that upon activation of the appropriate cell-surface receptors to stimulate PtdIns(3,4,5)P_3 synthesis, human PPIP5K1 translocates from the cytoplasm to the plasma membrane. We map a cryptic polyphosphoinositide-binding site in PPIP5Ks to an unusual hybrid domain, the N-terminal portion of a PH (pleckstrin homology) consensus sequence that is spliced into a phosphatase-like domain which itself has further evolved loss of catalytic function. This demonstration that PtdIns 3-kinase pathway can regulate compartmentalization of inositol pyrophosphate synthesis offers new opportunities to understand how signalling specificity can be controlled by cross-talk between signalling cascades. The present study is also of significance because, for the first time, we ascribe a physiologically relevant function to the so-called phosphatase-like domain of PPIP5K1, a topic that had previously generated considerable speculation [8,24].

MATERIALS AND METHODS

Protein expression and purification

PPIP5K1 kinase domain—The vector pGEX-4T-1 containing the cDNA encoding human GST (glutathione transferase)–PPIP5K1 was constructed exactly as described previously [8]. The construct was transformed into the ArcticExpress *Escherichia coli* strain (Stratagene) and grown in LB (Luria–Bertani) medium containing ampicillin (100 μg/ml) at 37 °C. When D_{600nm} was 0.7, cells were transferred to 10 °C and protein was induced for 24 h with 0.1 mM IPTG (isopropyl β-D-thiogalactopyranoside).

Cells were harvested by centrifugation and the pellets were resuspended in lysis buffer [25 mM Tris/HCl (pH 8.0), 350 mM NaCl, 1 mM DTT (dithiothreitol) and EDTA-free protease inhibitor mixture tablets (Roche Applied Science)]. After sonication (medium output; 6×10 s) and centrifugation (15 000 ***g*** at 4 °C for 30 min), the supernatant was loaded on to a 5 ml glutathione–Sepharose column (GE Healthcare Life Sciences), which was pre-equilibrated with lysis buffer. The protein was purified using an ÄKTA FPLC system (Amersham Bioscience) at 4 °C. The column was washed with 10 CV (column volumes) of buffer A [25 mM Tris/HCl (pH 8.0), 350 mM NaCl and 1 mM DTT] at 1 ml/min, followed by 2 CV of buffer B [25 mM Tris/HCl (pH 8.0), 50 mM NaCl and 1 mM DTT]. The final step was a gradient elution created by mixing buffer A with buffer C [25 mM Tris/HCl (pH 8.0), 50 mM NaCl, 1 mM DTT and 30 mM glutathione] using 0–100 % buffer C; 2 ml fractions of eluted protein were collected, mixed with 50 % glycerol and stored in aliquots at −80 °C.

PBD (polyphosphoinositide binding domain) 1 and PBD2—Full-length cDNAs for human *PPIP5K1* and human *PPIP5K2* [9] were used as templates for subcloning their acid-phosphatase-like domains, which we redesignate in the present study as PBDs (type 1, amino acids 382–917 of PPIP5K1; type 2, amino acids 371–901 of PPIP5K2). The PBDs were given C-terminal poly(His) tags using the pET-21a vector (EMD Chemicals). For

NIH-PA Author Manuscript

NIH-PA Author Manuscript

NIH-PA Author Manuscript

PBD1, the EcoRI 5′-primer was CGGAATTCCCCACCACATC-TGGCACTATG and the XhoI 3′-primer was CCGCTCGAG-CTCAACACCTTTCACTCC (the restriction sites are underlined). For PBD2 the EcoRI 5′-primer was CGGAATTCC-CAACTACATCTGGAACTATG and the XhoI 3′-primer was CCGCTCGAGTTCACAACCTTTGGCTCC. For PBD1^{R399A}, the mutational primer ATTGCAATTATT**GCT**CATGGGGATCGT (the mutagenic codon is depicted in bold font) and its corresponding reverse complement were used during the overlap extension PCR. The second mutant (PBD1^{R417A}) was generated in a similar way, using GTGAAACACCCA**GCT**TTTTTTGCTCTG and its reverse complement, along with the respective end primers mentioned above. All of the above constructs were transformed into DH5α cells for plasmid isolation and sequencing. Each of these constructs were transformed into the pGro7 chaperone-containing competent cells (Clontech), which were grown at 37 °C in LB containing 50 μg/ml ampicillin, 20 μg/ml chloramphenicol and 2 g of L-arabinose. When D_{600nm} was 0.6, the cells were transferred to 25 °C and protein was induced for 15 h with 1 mM IPTG. The cells were next collected by centrifugation (2400 ***g*** for 10 min at 4 °C), and resuspended in ice-cold lysis buffer containing 25 mM Hepes (pH 8), 300 mM NaCl, 10 mM imidazole, protease inhibitor cocktail tablets (one tablet per 10 ml of the buffer) and 0.1 % Triton X-100. The suspension was sonicated on ice (10 × 20 s). The lysate was cleared by centrifugation, filtered (0.22 μm pore) and 25 ml was added to 1 ml of Ni-NTA (Ni^{2+}-nitrilotriacetate)–agarose (Qiagen) for 40 min at 0–4 °C. The resin was then placed in a column, which was washed with 250 ml of 40 mM imidazole added to buffer A. This was followed by 10 ml of a second wash of buffer A plus 100 mM imidazole. Then, bound protein was eluted with 5 ml of buffer A plus 300 mM imidazole. The protein was next dialysed against buffer B and applied to a 5 ml HiTrap™ SP HP column (GE Healthcare) and eluted at 5 μl/min with buffer B plus a 0–100 %linear gradient of 2M NaCl, using an ÄKTA FPLC system.

Enzyme assays

All assays of inositol phosphate and inositol lipid metabolism were performed in lubricated microfuge tubes (PGC Scientifics). Kinase assays were performed by incubating the appropriate ^{3}H-labelled inositol phosphate substrate at 37 °C in buffer containing 1mM EDTA, 50 mM KCl, 20 mM Hepes (pH 7.2), 8 mM $MgSO_4$, 5 mM ATP and 10 mM NaF. All of the phosphatase assays were performed by incubating the appropriate ^{3}H-labelled inositol phosphate substrate [or C_8PtdIns(3,4,5)P_3] at 37 °C in buffer containing 1 mM EDTA and 5 mM Hepes (pH 7.2), with 100 mM KCl, 2 mM $MgCl_2$ and 0.5 mg/ml BSA.

The degree of PtdIns(3,4,5)P_3 hydrolysis was recorded by assaying phosphate release [25]. For the inositol phosphate assays, these were acid quenched (0.2 volumes 2 M perchloric acid and 1 mg/ml InsP_6), neutralized and analysed by Partisphere SAX HPLC as described previously [5]. Usually, the ^{3}H in individual 1 ml fractions was determined after mixing with 4 ml of MonoFlow 4 scintillant (National Diagnostics), although occasionally a Flo-1 in-line radioactivity detector (Radiomatic Instruments) was used. Recovery of ^{3}H in all assays was >85 % and did not vary with the degree of metabolism, indicating that there was no systematic loss of any particular product.

The hydrolysis of *p*-nitrophenyl phosphate was studied in the phosphatase assay buffer (see above), except that EDTA was omitted. At the end of each incubation period, the reaction was stopped by the addition of 1 M NaOH and the absorbance of the resulting solution at 405 nm was recorded with a SpectraMax 340 microplate spectrophotometer (Molecular Devices).

NIH-PA Author Manuscript

NIH-PA Author Manuscript

NIH-PA Author Manuscript

PEG (polyethylene glycol) precipitation

This assay is based on methods that were used in a previous study [26]. PBD2 (32 μg) was incubated at 4 °C for 20 min in 50 μl of buffer containing 25 mM Hepes (pH 7.2), 5 mg/ml bovine γ-globulin, 100 mM KCl, 1 mM EDTA, 1 mM DTT, [^{3}H]InsP$_6$ (approx. 15000 d.p.m.) and increasing amounts of non-radioactive InsP$_6$ (or C$_8$-PtdIns(3,4,5)P$_3$; Cabiochem. Then 35 μl of ice-cold 30 % (w/v) PEG was added, with vortexing, followed by 10 min at 0–4 °C. Samples were subsequently centrifuged at 10 000 ***g*** (10 min at 4 °C). The supernatants were removed (and saved for counting free [^{3}H]InsP$_6$) and the resulting pellet was carefully washed with 1 ml of the incubation buffer (but without ligand or bovine γ-globulin). The pellet and protein-bound [^{3}H]InsP$_6$ was resuspended in 1 ml of 1 % SDS and 8 ml of Monoflow scintillation fluid.

SPR (surface plasmon resonance)

The Biacore sensor chip Pioneer L1 was used for immobilizing large unilamellar vesicles [77:20:3 by vol. PtdCho (phosphatidylcholine)/PtdE (phosphatidylethanolamine)/test phosphoinositide] [27], as described previously [28]. Then, 90 μl of the vesicles were injected over the chip surface at a flow rate of 5 μl/min until the response reached 5000 RU (response units). The protein under study was injected at a flow rate of 5 μl/min in buffer containing 100 mM KCl, 6 mM MgCl$_2$, 5 mM Na$_2$ATP and 25 mM Hepes (pH 7.2). The RU in the resulting sensorgram were automatically corrected for any response arising from protein interacting with control vesicles from which the test phosphoinositide was omitted. The values of the saturating RU (R_{eq}) were plotted against the protein concentrations (C) and the equilibrium binding affinity (K_d) was subsequently determined by performing a non-linear least-squares analysis of the binding isotherm using the equation $R_{eq}=R_{max}/(1+K_d/C)$, where R_{max} is the maximal R_{eq} value. The S.E.M. of individual R_{eq} determinations did not exceed 1 % of the mean values.

Confocal immunofluorescence

NIH 3T3 cells were seeded on to 35 mm glass bottom micro-well dishes and transfected 24 h later with cDNA coding FLAG-PPIP5K1 (cloned into the pDEST515 plasmid) using Lipofectamine™ 2000 (Invitrogen) according to the manufacturer's instructions. On the following day, cells were serum starved for 3 h and treated as indicated with 50 ng/ml PDGF (platelet-derived growth factor; Sigma). For immunostaining, cells were rinsed twice with PBS, fixed with 3 %paraformaldehyde in PBS containing 4 % sucrose for 15 min at room temperature (23 °C), permeabilized with 0.2 % Triton X-100 for 5 min and washed with PBS. After blocking with 10 % (v/v) BSA/PBS for 30 min at 37 °C, cells were incubated with the primary antibody (mouse monoclonal anti-FLAG, Abcam #ab18230) for 2 h at 37 °C and washed with PBS, followed by 1 h incubation at 37 °C with the secondary antibody (Alexa Fluor® 488 goat anti-mouse; Invitrogen #A-11001) and washed with PBS before incubation with DAPI (4′,6-diamidino-2-phenylindole; Invitrogen, #D1306) for 10 min at 37 °C. After washing the cells twice with PBS, confocal images were taken on a Zeiss LSM 510 META using a Plan-Apochromat ×63/1.4 oil objective. The cellular distribution of the FLAG-PPIP5K1 was recorded by line intensity profiles [29] using LSM Image Examiner software. Data were exported into SigmaPlot and the ratios of pixel intensity (plasma membrane/cytoplasm) were then calculated as described previously [30].

Other materials

[^{3}H]InsP$_6$ was purchased from PerkinElmer and was purified by HPLC using a 4 mm×250 mm IonPac AS7 column (Dionex) eluted with a linear gradient of 0–1 M nitric acid. Fractions containing pure [^{3}H]InsP$_6$ were saved and lyophilized. 5-PP-[^{3}H]InsP$_5$, 1/3-PP-[^{3}H]InsP$_5$ and 1/3,5-[PP]$_2$-[^{3}H]InsP$_4$ were prepared as previously described [5,9,31]. All of

NIH-PA Author Manuscript

NIH-PA Author Manuscript

NIH-PA Author Manuscript

the restriction enzymes were purchased from New England Biolabs. All of the phospholipids (1-stearoyl-2-arachidonoyl) were purchased from Avanti Polar Lipids. Non-radioactive $InsP_6$ was purchased from Calbiochem. CHAPS, octyl glucoside, LY294002 and L-arabinose were purchased from Sigma–Aldrich. The GRP-1 (general receptor for phosphoinositides-1) PH domain construct was provided by Dr David Lambright (University of Massachusetts Medical School, Worcester, MA, U.S.A.) [32]; it was expressed and purified as previously described [33]. The protease inhibitor cocktail tablets were bought from Roche Applied Science and the Pioneer L1 Biacore sensor chip was purchased from GE Healthcare Life Sciences. Recombinant hMIPP (human multiple inositol polyphosphate phosphatase) was expressed and purified as previously described [34].

RESULTS

The catalytic activity of the kinase domain of PPIP5K1

Mammalian PPIP5Ks, and the yeast homologue Vip1, have previously been shown to phosphorylate both $InsP_6$ and 5-PP-$InsP_5$ [5,8–10] and thereby participate in two pathways of $[PP]_2$-$InsP_4$ synthesis (Figure 1A), here named ‘I’ and ‘II’, as in an earlier study [35]. The kinase activity is self-contained in the N-terminal third of the Vip1/PPIP5Ks (Figure 1 and [8]). Fridy et al. [8], previously determined that the catalytic specificity of this kinase domain for 5-PP-$InsP_5$ is 2.5-fold higher than the corresponding value for $InsP_6$. A much greater (80-fold) catalytic preference for 5-PP-$InsP_5$ was observed in our experiments (Table 1). This catalytic preference of the kinase for 5-PP-$InsP_5$ can be predicted to be less dramatic *in vivo*, where the cellular levels of $InsP_6$ substantially exceed those of 5-PP-$InsP_5$ (Table 1). However, if there were to be any compartmentalization of PPIP5K within a single cell, there could be a localized metabolism of either of these alternate substrates.

We noted (Figure 1D) that the kinase domain can further phosphorylate the 1/3-PP-$InsP_5$ to a compound that we have designated as an $InsP_8$, since it co-elutes with $[PP]_2$-$InsP_4$ (which also has eight phosphates). Some further phosphorylation to $InsP_9$ was also observed (Figure 1D). Vip1 can also convert 1/3-PP-$InsP_5$ into $InsP_8$ and $InsP_9$; such molecules, which were speculated to contain triphosphate groups, have been suggested to significantly expand the family of diphosphoinositol polyphosphates [36]. It was further indicated [36] that such molecules are acid-labile and might degrade during acid-based cell lysis, or even during their HPLC separation; if so, this could have led us to significantly underestimate the efficiency of 1/3-PP-$InsP_5$ phosphorylation. To check this possibility, we HPLC-purified $^3HInsP_8$ and then took this material through another round of our acid-quench, neutralization and HPLC procedures. We recovered >85 % of the $InsP_8$ and we did not detect any dephosphorylation of this compound. We are therefore confident that we have accurately determined that the catalytic efficiency of 1/3-PP-$InsP_5$ phosphorylation by PPIP5K1 is very low (Table 1) and of doubtful biological significance. Ins(1,3,4,5,6)P_5 was another relatively weak substrate (Table 1); the 2-phosphate group presumably makes a significant contribution to substrate specificity. We conclude that the physiological substrates for phosphorylation by PPIP5K1 are $InsP_6$ and 5-PP-$InsP_5$.

The phosphatase-like domains of PPIP5K1 and PPIP5K2 do not express phosphatase activity

Previous molecular modelling studies [10] have identified the central third portion of Vip1/PPIP5Ks as a putative acid-phosphatase domain (see Figure 5). In particular, these domains contain the RHGXRXP catalytic motif which, in phytases [37] and hMIPP [38], is specialized for the hydrolysis of $InsP_6$ and other inositol phosphates. There has therefore been considerable speculation concerning what might be the function of this domain in Vip/PPIP5Ks [8,24]. We have previously shown [9] that *in vitro* full-length recombinant human

NIH-PA Author Manuscript

NIH-PA Author Manuscript

NIH-PA Author Manuscript

PPIP5K1 does not de-phosphorylate either Ins(1,3,4,5,6)P_5, InsP_6, 5-PP-InsP_5 or $[PP]_2$-InsP_4. In the present study, we examined whether the phosphatase-like domains from each protein would possess catalytic activity. This reductionist approach is more sensitive because we were able to express in *E. coli* larger quantities of the domains at higher purity than we could achieve with full-length proteins. The phosphatase-like domain of PPIP5K1 was incubated for up to 15 h at 37 °C with InsP_6 (Figure 2A), or 5-PP-InsP_5 (Figure 2B), or either 1/3-PP-InsP_5, $[PP]_2$-InsP_4 or the putative InsP_8 triphosphate (results not shown; all assays used trace amounts of ^{3}H-labelled material and in additional assays with InsP_6 we used 1 μM amounts); none of these polyphosphates were hydrolysed. Identical results were obtained with the phosphatase-like domain of PPIP5K2 (results not shown). We additionally incubated the phosphatase-like domains of either PPIP5K1 or PPIP5K2 with *p*-nitrophenyl phosphate, a generic substrate for all acid phosphatases; again, there was no activity (Figure 2C). In contrast, when added at a similar concentration to that of the PPIP5Ks, hMIPP [38] hydrolysed *p*-nitrophenyl phosphate at a rate of approx. 10 nM/mg of protein per min (Figure 2C). We conclude that these phosphatase-like domains are catalytically inactive.

The phosphatase-like domain of PPIP5K1 binds InsP_6 and PtdIns(3,4,5)P_3

In addition to the substrate binding domain that is constructed around the RHGXRXP motif, acid phosphatases utilize a remote and catalytically essential histidine to hydrolyze substrate. This histidine normally occurs as a His-Asp dipeptide [37] (or His-Ala-Glu tripeptide in the specific case of hMIPP [38]). The absence in the phosphatase-like domains of such a histidine in the appropriate context [8] could help explain our demonstration that this domain lacks phosphatase activity. So what could be the functional significance of the tight conservation of the RHGXRXP motif? To answer that question, we investigated whether the phosphatase-like domain is important in binding of ligand, rather than its metabolism. We first examined whether the phosphatase-like domain of PPIP5K2 would bind InsP_6. After equilibration of InsP_6 with the domain, we separated bound and free ligand by precipitating protein with PEG [39]. In these experiments, InsP_6 was found to bind to the protein (K_d = 0.6 μM; Figure 3).

The binding of InsP_6 to certain proteins does not always involve a specific recognition of the three-dimensional pattern of phosphate groups around the inositol ring. Instead, because of its especially high concentration of electronegative charge around the inositol ring, InsP_6 can interact with some proteins through non-specific delocalized electrostatic interactions, particularly to proteins with an electrostatically polarized region such as a PH domain [40]. However, the most biologically relevant ligands for PH domains are usually the inositol lipids [40]. These considerations led us to directly compare InsP_6-and PtdIns(3,4,5)P_3-binding to the phosphatase-like domain of PPIP5K2. In PEG-precipitation assays, a C_8 soluble analogue of PtdIns(3,4,5)P_3 was 2- to 3-fold more potent than InsP_6 itself at displacing ^{3}HInsP_6 from the domain (Figure 3). That is, these assays indicate that PtdIns(3,4,5)P_3 is the preferred ligand. This is also likely to be case *in vivo* after activation of the PtdIns 3-kinase pathway, which can elevate PtdIns(3,4,5)P_3 levels to approx. 200 μM [41], well above InsP_6 levels (Table 1). These considerations, and the further experiments described below, have led us to re-designate this region of the PPIP5K proteins as a PBD.

The PtdIns(3,4,5)P_3-binding affinities of the PBDs of PPIP5K1 and PPIP5K2

To more rigorously define phosphoinositide recognition by the PBD domains of PPIP5K1 and PPIP5K2, we measured equilibrium binding by SPR [27,28]. To maximize biological relevance, these experiments were performed in buffer containing 100 mM KCl, 1 mM free Mg^{2+} and 5 mM MgATP. We utilized membrane mimetics, that is we immobilized phospholipid vesicles made from PtdCho and PtdE into which we incorporated 3 %(v/v) PtdIns(3,4,5)P_3 [27]. As a control, we first examined the binding of the GRP-1 PH domain

NIH-PA Author Manuscript

NIH-PA Author Manuscript

NIH-PA Author Manuscript

to these vesicles. Sensorgrams were obtained at several different protein concentrations (Figure 4A), from which equilibrium binding affinity was determined (Figure 4B). The K_d value that we obtained for the GRP-1-PH (59 nM) is within the range of values published by others using the same technique (28–170 nM; [33,42]).

We next determined the affinity with which PtdIns(3,4,5)P_3 binds to the newly renamed PBD domains of the PPIP5Ks (Figure 4). PBD1 bound PtdIns(3,4,5)P_3 with high affinity (K_d = 96 nM; Figures 4C and 4D). This affinity is within the range of values that has previously been determined for a subset of PH domains, including GRP-1 (see above), that are specialized for binding to PtdIns(3,4,5)P_3 [27,33]. We also found that PtdIns(3,4,5)P_3 is a ligand for PBD2 (Figures 4E and 4F), but with considerably lower affinity (K_d = 705 nM; Figure 4F) than that for PBD1.

The data described above demonstrate that the PBDs are catalytically inactive against inositol phosphates and even *p*-nitrophenyl phosphate, a generic acid-phosphatase substrate. Nevertheless, in view of the high affinity of these domains for PtdIns(3,4,5)P_3 (see above) we also incubated PBD1 (35 μg/ml) for 24 h at 37 °C with 1 mM of the C_8 soluble analogue of PtdIns(3,4,5)P_3. Using a sensitive phosphate release assay [25], we were unable to detect any hydrolysis of the lipid (results not shown).

The nature of the PBDs: novel, hybrid domains

The amino acid sequences of the PBD domains of PPIP5K1 and PPIP5K2 were aligned with two related InsP_6-metabolizing acid phosphatases, namely the hMIPP [38] and an *E. coli* phytase. This alignment identifies an approx. 30 amino acid residue insert, beginning immediately C-terminal of the RHGXRXP motif in the PBDs, which does not correspond to the genuine acid phosphatase sequences (Figure 5A). This insert in the PDBs, in separate alignments (Figure 5B), was found to be similar in several respects to the N-terminal portion of PtdIns(3,4,5)P_3-specific PH domains [43]: for example (Figure 5B), the second β-strand of such PH domains has an R/KXRXF/L motif [43] that is well conserved in PBD1 (HXRXF), although slightly less conserved in PBD2 (HXKXF). Additionally, a tyrosine residue that is frequently present in the third β-strand of the PH domain [43] was aligned with a tyrosine in PBD1 and PBD2 (Figure 5B). Some additional similarities between the PBD insert and the PtdIns(3,4,5)P_3-binding subset of PH domains are highlighted in Figure 5(B). Furthermore, in PPIP5Ks, just before the N-terminus of the putative PH domain insert, the first arginine in the RHGXRXP phosphatase motif aligns with a conserved lysine in the first β-strand of these PH domains (Figure 5B). That is, an unusual hybrid motif within PBDs aligns with a partial PH domain consensus. We experimentally tested the significance of these alignments by mutagenesis of two residues in PBD1 (corresponding to Arg^{399} and Arg^{417} in full-length PPIP5K1, marked by arrows in Figure 5B). These electropositive amino acids are good candidates for binding to the negatively charged phosphates in the headgroup of PtdIns(3,4,5)P_3. The K_d values for the binding of PtdIns(3,4,5)P_3 by PBD1R399A and PBD1R417A mutants were 8-fold and 16-fold lower than the K_d values for the wild-type PBD1, confirming the functionality of these two arginine residues (Figure 6). Arg^{399} in PBD1 is conservatively replaced with a lysine in PBD2 (Figure 5), which might contribute to the latter's lower affinity for PtdIns(3,4,5)P_3 (Figure 4). Note that Vip1, the yeast homologue of the PPIP5Ks, cannot bind PtdIns(3,4,5)P_3 *in vivo*, as this lipid is not synthesized by that organism. Could Vip1 bind PtdIns(4,5)P_2 instead? We have not directly answered that question, but we note that Vip1 lacks a residue equivalent to Arg^{417} in PBD1 (Figure 5). Mutagenesis of this particular arginine in PBD1 eliminated all detectable binding of PtdIns(4,5)P_2 (results not shown). Our data therefore predict that Vip1 is unlikely to bind to inositol lipids *in vivo*.

NIH-PA Author Manuscript

NIH-PA Author Manuscript

NIH-PA Author Manuscript

The specificity of lipid binding to the PBDs of PPIP5K1 and PPIP5K2

PBD1 was found to bind PtdIns(4,5)P_2 and PtdIns(3,4)P_2 with approx. 6-fold lower affinity than does PtdIns(3,4,5)P_3 (Figures 7A–7D). These data indicate that both the 3- and 5-phosphates of PtdIns(3,4,5)P_3 contribute to ligand affinity. However, there was no significant binding of PtdIns(3,5)P_2 to PBD1 (results not shown). This observation that polyphosphoinositide binding requires vicinal phosphate groups is known to be a characteristic of the PH domain [44]. Ptd3P, Ptd4P and Ptd5P did not bind to PBD1 (results not shown). PBD2 bound PtdIns(4,5)P_2 relatively weakly (Figures 7E and 7F) and did not bind PtdIns(3,5)P_2, Ptd3P, Ptd4P or Ptd5P (results not shown). Clearly, PBD1 has a considerably greater affinity for inositol lipids than does PBD2 (Figures 4 and 7).

In intact cells, PPIP5K1 translocates to plasma membranes after activation of the PtdIns 3-kinase signalling pathway

The experiments described above demonstrate that PPIP5K1 contains a domain (PBD1) that binds PtdIns(3,4,5)P_3 and, with a 6-fold lower affinity, PtdIns(4,5)P_2. We therefore next examined the intracellular distribution of PPIP5K1 in NIH 3T3 cells. To maximize the physiological relevance of these experiments, we transfected the cells with full-length human PPIP5K1 (FLAG-tagged), rather than just the protein's PBD domain. The intracellular distribution of the protein was monitored by confocal immunofluorescence (Figure 8).

Representative examples of single cells are shown in Figure 8. The data were quantified by recording line intensity profiles [29] from which the ratios of pixel intensity (plasma membrane/cytoplasm) were calculated ([30]; Figures 8A and 8D). We found that PPIP5K1 was distributed throughout the cytoplasm, although a slightly elevated level of PPIP5K1 was found at the plasma membrane (Figures 8A and 8D). This may reflect some binding of PPIP5K1 to PtdIns(4,5)P_2, but, given that we studied localization of the full-length protein, there may be additional protein–protein interactions.

PtdIns(3,4,5)P_3 is a plasmalemmal second messenger, the levels of which increase dramatically after receptor-dependent activation of the PtdIns 3-kinase pathway [41]. Upon 5 min of treatment of NIH 3T3 cells with PDGF, a PtdIns 3-kinase activator, there was a significant increase in the proportion of PPIP5K1 that was present at the plasma membrane (Figure 8). This translocation of PPIP5K1 was largely prevented when the PtdIns 3-kinase pathway was inhibited by pre-treatment of cells with LY294002 (Figures 8C and 8D). Thus the PtdIns 3-kinase pathway enhances compartmentalization of inositol pyrophosphate synthesis *in vivo*.

DISCUSSION

The purification and cloning of the PPIP5K family [8,9] (Vip1 in yeasts [10]) solved a long-standing problem in the inositol pyrophosphate field: the identification of the enzymes that synthesize [PP]$_2$-InsP_4 from PP-InsP_5. However, this development brought with it an unexpected conundrum. In addition to a kinase domain, the Vip1/PPIP5K proteins were found to contain a region with similarities in amino acid sequence to certain acid phosphatases (such as phytase and MIPP) that are specialized for the dephosphorylation of inositol phosphates. The presence of competing phosphatase and kinase activities within a single protein is rare, but of considerable significance when it occurs [45]. However, one of the achievements of our present study is to demonstrate that this domain is not a functional phosphatase, but instead it is shown to be specialized for binding of inositol lipids. Our experiments also indicate that the lipid-binding site is formed from a novel hybrid sequence constructed from partial PH and acid-phosphatase domains. We further show that the

NIH-PA Author Manuscript

NIH-PA Author Manuscript

NIH-PA Author Manuscript

activation of the PtdIns 3-kinase pathway is associated with PPIP5K1 translocation to the plasma membrane. This new observation of a mechanism for receptor-dependent compartmentalization of inositol pyrophosphate synthesis represents another important finding in the present study.

Multiple sequence alignments provide evidence that the PtdIns(3,4,5)P_3-binding region of PPIP5Ks, the PBDs, includes a partial PH domain (Figure 5). This conclusion is supported by our characterization of the specificity of inositol lipid binding to these domains: PtdIns(4,5)P_2 and PtdIns(3,4)P_2, which both have vicinal phosphates, were shown to bind to the PBD1 albeit with weaker affinity than did PtdIns(3,4,5)P_3. In contrast, neither PtdIns(3,5)P_2 nor any of the PtdInsPs exhibited any significant binding to PBDs (see the Results section). Thus, just like other PH domains that preferentially bind PtdIns(3,4,5)P_3, PBDs demonstrates an absolute requirement for two vicinal phosphate groups [44]. Moreover, Arg^{417} in the PBD of PPIP5K1 was shown by mutagenesis to make a critical contribution to ligand binding (Figure 6). This arginine residue aligns with a conserved arginine in the second β-strand of certain PH domains (Figure 5), which also participates in ligand binding [43]. It is also intriguing that a conserved and functionally important lysine residue in the first β-strand of the PH domain [43] was aligned with the first arginine residue in the RHGXRXP phosphatase motif within the PBDs (Figure 5). Our mutagenic experiments revealed that this residue, Arg^{399}, also makes a significant contribution to ligand binding in PPIP5K1 (Figure 6). Thus we conclude that the PBD may be considered a novel hybrid domain.

It is possible that the presence of this PH domain-like insert may contribute to the phosphatase-like sequence being catalytically inactive, but in addition previous alignments [8] have shown that PPIP5Ks lack a remote histidine that is catalytically essential in genuine acid phosphatases such as phytases and MIPP [37,38]. In any case, we believe that the new findings in the present study, together with our earlier work [9], should end speculation [8,24] that PPIP5Ks might harbour phosphatase activity. To reiterate all of our findings on this topic: in earlier work [9], the levels of inositol phosphates in HEK (human embryonic kidney) cells were unchanged following overexpression of a kinase-dead mutant of full-length PPIP5K1. That is an experimental paradigm that would be expected to unmask any significant phosphatase activity. Furthermore, the full-length recombinant PPIP5K1 does not dephosphorylate either Ins(1,3,4,5,6)P_5, InsP_6, 5-PP-InsP_5 or $[PP]_2$-InsP_4 [9]. In the present study, the latter polyphosphates were again demonstrated not to be substrates, but now our conclusion is more rigorous because we incubated the PBDs from both PPIP5K1 and PPIP5K2 at higher concentrations and for longer times than in previous experiments with full-length PPIP5K1. Finally, we have extended the list of molecules that are not substrates to also include 1/3-PP-InsP_5, InsP_8 (a putative triphosphate, see [36]), PtdIns(3,4,5)P_3 and even *p*-nitrophenyl phosphate, a generic acid-phosphatase substrate.

One of the most important mechanisms for achieving signalling specificity by a particular pathway is through regulated spatial organization of its key components [46]. Our present study shows that this is a property of the inositol pyrophosphate signalling cascade. Inositol lipid-dependent compartmentalization of PPIP5K1 in animal cells is significant because it provides a novel means of regulating inositol phosphate signalling pathways. Thus it seems likely there can be PtdIns 3-kinase-dependent localized elevations in the concentrations of the products of 1/3-PP-InsP_5 and $[PP]_2$-InsP_4 (Figure 1 and Table 1). This indication that under certain circumstances inositol pyrophosphate synthesis can be compartmentalized adds new features to our understanding of the mechanisms of action of inositol pyrophosphates. As outlined in the Introduction section, irrespective of whether these pyrophosphates act by transphosphorylating proteins or by binding to specific receptors, compartmentalization of inositol pyrophosphate synthesis can enhance their biological

NIH-PA Author Manuscript

NIH-PA Author Manuscript

NIH-PA Author Manuscript

activities. Exocytosis is at least one plasma membrane located event that is regulated by inositol pyrophosphates [47]. Nevertheless, the importance of compartmentalization of PPIP5K may well go beyond local elevations in inositol pyrophosphate concentrations. Perhaps translocation of PPIP5K1 to the plasma membrane modifies its kinase activity. Additionally, PPIP5K might engage in functionally significant, but non-catalytic, protein–protein interactions. The exceptionally high-affinity binding of PPIP5K to PtdIns(3,4,5)P_3 (Figure 4) could also prohibit or displace the binding to this lipid of other proteins that might have lower affinity for PtdIns(3,4,5)P_3; such ligand competition could also have regulatory significance. One or more of these options are likely to be productive directions for future research into the biological significance of the PPIP5K family.

Acknowledgments

We thank Agnes Janoshazi and Jeff Tucker for assistance with the confocal microscopy and for data evaluation.

FUNDING

This work was supported by the Intramural Research Program of the National Institutes of Health/National Institute of Environmental Health Sciences.

Abbreviations used

CV	column volumes
DTT	dithiothreitol
GRP-1	general receptor for phosphoinositides-1
IP6K	$InsP_6$ kinase
hMIPP	human multiple inositol polyphosphate phosphatase
IPTG	isopropyl β-D-thiogalactopyranoside
LB	Luria–Bertani
PBD	polyphosphoinositide binding domain
PDGF	platelet-derived growth factor
PEG	polyethylene glycol
PH	pleckstrin homology
PPIP5K	PP-$InsP_5$ kinase
PtdCho	phosphatidylcholine
PtdE	phosphatidylethanolamine
RU	response units
SPR	surface plasmon resonance

References

1. Seeds AM, York JD. Inositol polyphosphate kinases: regulators of nuclear function. Biochem Soc Symp. 2007; 74:183–197. [PubMed: 17233590]
2. Barker CJ, Illies C, Gaboardi GC, Berggren PO. Inositol pyrophosphates: structure, enzymology and function. Cell Mol Life Sci. 2009; 66:3851–3871. [PubMed: 19714294]
3. Burton A, Hu X, Saiardi A. Are inositol pyrophosphates signalling molecules? J Cell Physiol. 2009; 220:8–15. [PubMed: 19326391]

NIH-PA Author Manuscript

NIH-PA Author Manuscript

NIH-PA Author Manuscript

4. Shears SB. Diphosphoinositol polyphosphates: metabolic messengers? Mol Pharmacol. 2009; 76:236–252. [PubMed: 19439500]
5. Lin H, Fridy PC, Ribeiro AA, Choi JH, Barma DK, Vogel G, Falck JR, Shears SB, York JD, Mayr GW. Structural analysis and detection of biological inositol pyrophosphates reveals that the VIP/PPIP5K family are 1/3-kinases. J Biol Chem. 2009; 284:1863–1872. [PubMed: 18981179]
6. Saiardi A, Nagata E, Luo HR, Snowman AM, Snyder SH. Identification and characterization of a novel inositol hexakisphosphate kinase. J Biol Chem. 2001; 276:39179–39185. [PubMed: 11502751]
7. Draskovic P, Saiardi A, Bhandari R, Burton A, Ilc G, Kovacevic M, Snyder SH, Podobnik M. Inositol hexakisphosphate kinase products contain diphosphate and triphosphate groups. Chem Biol. 2008; 15:274–286. [PubMed: 18355727]
8. Fridy PC, Otto JC, Dollins DE, York JD. Cloning and characterization of two human VIP1-like inositol hexakisphosphate and diphosphoinositol pentakisphosphate kinases. J Biol Chem. 2007; 282:30754–30762. [PubMed: 17690096]
9. Choi JH, Williams J, Cho J, Falck JR, Shears SB. Purification, sequencing, and molecular identification of a mammalian PP-InsP5 kinase that is activated when cells are exposed to hyperosmotic stress. J Biol Chem. 2007; 282:30763–30775. [PubMed: 17702752]
10. Mulugu S, Bai W, Fridy PC, Bastidas RJ, Otto JC, Dollins DE, Haystead TA, Ribeiro AA, York JD. A conserved family of enzymes that phosphorylate inositol hexakisphosphate. Science. 2007; 316:106–109. [PubMed: 17412958]
11. Albert C, Safrany ST, Bembenek ME, Reddy KM, Reddy KK, Falck JR, Bröker M, Shears SB, Mayr GW. Biological variability in the structures of diphosphoinositol polyphosphates in *Dictyostelium discoideum* and mammalian cells. Biochem J. 1997; 327:553–560. [PubMed: 9359429]
12. Lee YS, Huang K, Quiocho FA, O'Shea EK. Molecular basis of cyclin-CDK–CKI regulation by reversible binding of an inositol pyrophosphate. Nat Chem Biol. 2008; 4:25–32. [PubMed: 18059263]
13. Lee YS, Mulugu S, York JD, O'Shea EK. Regulation of a cyclin-CDK–CDK inhibitor complex by inositol pyrophosphates. Science. 2007; 316:109–112. [PubMed: 17412959]
14. Bhandari R, Saiardi A, Ahmadibeni Y, Snowman AM, Resnick AC, Kristiansen TZ, Molina H, Pandey A, Werner JK Jr , Juluri KR, et al. Protein pyrophosphorylation by inositol pyrophosphates is a post-translational event. Proc Natl Acad Sci USA. 2007; 104:15305–15310. [PubMed: 17873058]
15. Saiardi A, Bhandari A, Resnick R, Cain A, Snowman AM, Snyder SH. Inositol pyrophosphate: physiologic phosphorylation of proteins. Science. 2004; 306:2101–2105. [PubMed: 15604408]
16. Azevedo C, Burton A, Ruiz-Mateos E, Marsh M, Saiardi A. Inositol pyrophosphate mediated pyrophosphorylation of AP3B1 regulates HIV-1 Gag release. Proc Natl Acad Sci USA. 2009; 106:21161–21166. [PubMed: 19934039]
17. Houslay MD. Underpinning compartmentalised cAMP signalling through targeted cAMP breakdown. Trends Biochem Sci. 2010; 35:91–100. [PubMed: 19864144]
18. Nezu A, Tanimura A, Morita T, Tojyo Y. Visualization of Ins(1,4,5)P3 dynamics in living cells: two distinct pathways for Ins(1,4,5)P3 generation following mechanical stimulation of HSY-EA1 cells. J Cell Sci. 2010; 123:2292–2298. [PubMed: 20554898]
19. Brehm MA, Schenk TM, Zhou X, Fanick W, Lin H, Windhorst S, Nalaskowski MM, Kobras M, Shears SB, Mayr GW. Intracellular localization of human inositol (1,3,4,5,6)-P_5 2-kinase. Biochem J. 2007; 408:335–345. [PubMed: 17705785]
20. Nalaskowski MM, Deschermeier C, Fanick W, Mayr GW. The human homologue of yeast ArgRIII protein is an inositol phosphate multikinase with predominantly nuclear localization. Biochem J. 2002; 366:549–556. [PubMed: 12027805]
21. Schell MJ, Irvine RF. Calcium-triggered exit of F-actin and IP_3 3-kinase A from dendritic spines is rapid and reversible. Eur J Neurosci. 2006; 24:2491–2503. [PubMed: 17100838]
22. Yang L, Reece J, Gabriel SE, Shears SB. Apical localization of ITPK1 enhances its ability to be a modifier gene product in a murine tracheal cell model of cystic fibrosis. J Cell Sci. 2006; 119:1320–1328. [PubMed: 16537650]

NIH-PA Author Manuscript

NIH-PA Author Manuscript

NIH-PA Author Manuscript

23. Otto JC, Kelly P, Chiou ST, York JD. Alterations in an inositol phosphate code through synergistic activation of a G protein and inositol phosphate kinases. Proc Natl Acad Sci USA. 2007; 104:15653–15658. [PubMed: 17895383]
24. Pohlmann J, Fleig U. Asp1, a conserved 1/3 inositol polyphosphate kinase, regulates the dimorphic switch in *S. pombe*. Mol Cell Biol. 2010; 30:4535–4547. [PubMed: 20624911]
25. Hoenig M, Lee RJ, Ferguson DC. A microtiter plate assay for inorganic phosphate. J Biochem Biophys Methods. 1989; 19:249–252. [PubMed: 2555407]
26. Ye W, Ali N, Bembenek ME, Shears SB, Lafer EM. Inhibition of clathrin assembly by high-affinity binding of specific inositol polyphosphates to the synapse-specific clathrin assembly protein AP-3. J Biol Chem. 1995; 270:1564–1568. [PubMed: 7829485]
27. Narayan K, Lemmon MA. Determining selectivity of phosphoinositide-binding domains. Methods. 2006; 39:122–133. [PubMed: 16829131]
28. Gokhale NA, Abraham A, Digman MA, Gratton E, Cho W. Phosphoinositide specificity of and mechanism of lipid domain formation by annexin A2-p11 heterotetramer. J Biol Chem. 2005; 280:42831–42840. [PubMed: 16230353]
29. Balla T, Varnai P. Visualizing cellular phosphoinositide pools with GFP-fused protein-modules. Sci STKE. 2002; 2002:L3.
30. Marechal Y, Pesesse X, Jia Y, Pouillon V, Perez-Morga D, Daniel J, Izui S, Cullen PJ, Leo O, Luo HR, et al. Inositol 1,3,4,5-tetrakisphosphate controls proapoptotic *Bim* gene expression and survival in B cells. Proc Natl Acad Sci USA. 2007; 104:13978–13983. [PubMed: 17709751]
31. Caffrey JJ, Safrany ST, Yang X, Shears SB. Discovery of molecular and catalytic diversity among human diphosphoinositol polyphosphate phosphohydrolases: an expanding NUDT family. J Biol Chem. 2000; 275:12730–12736. [PubMed: 10777568]
32. Lietzke SE, Bose S, Chawla A, Czech MP, Lambright DG. Structural basis of 3-phosphoinositide recognition by pleckstrin homology domains. Mol Cell. 2000; 6:385–394. [PubMed: 10983985]
33. Manna D, Albanese A, Park WS, Cho W. Mechanistic basis of differential cellular responses of phosphatidylinositol 3,4-bisphosphate- and phosphatidylinositol 3,4,5-trisphosphate-binding pleckstrin homology domains. J Biol Chem. 2007; 282:32093–32105. [PubMed: 17823121]
34. Cho J, King JS, Qian X, Harwood AJ, Shears SB. Dephosphorylation of 2,3-bisphosphoglycerate by MIPP expands the regulatory capacity of the Rapoport–Luebering glycolytic shunt. Proc Natl Acad Sci USA. 2008; 105:5998–6003. [PubMed: 18413611]
35. Padmanabhan U, Dollins DE, Fridy PC, York JD, Downes CP. Characterization of a selective inhibitor of inositol hexakisphosphate kinases: use in defining biological roles and metabolic relationships of inositol pyrophosphates. J Biol Chem. 2009; 284:10571–10582. [PubMed: 19208622]
36. Losito O, Szijgyarto Z, Resnick AC, Saiardi A. Inositol pyrophosphates and their unique metabolic complexity: analysis by gel electrophoresis. PloS ONE. 2009; 4:e5580. [PubMed: 19440344]
37. Rao DE, Rao KV, Reddy TP, Reddy VD. Molecular characterization, physicochemical properties, known and potential applications of phytases: an overview. Crit Rev Biotechnol. 2009; 29:182–198. [PubMed: 19514894]
38. Caffrey JJ, Hidaka K, Matsuda M, Hirata M, Shears SB. The human and rat forms of multiple inositol polyphosphate phosphatase: functional homology with a histidine acid phosphatase up-regulated during endochondral ossification. FEBS Lett. 1999; 442:99–104. [PubMed: 9923613]
39. Theibert AB, Estevez VA, Ferris C, Danoff SK, Barrow RK, Prestwich GD, Snyder SH. Inositol 1,3,4,5–tetrakisphosphate and inositol hexakisphosphate receptor proteins: isolation and characterization from brain. Proc Nat Acad Sci USA. 1991; 88:3165–3169. [PubMed: 1849645]
40. Lemmon MA, Ferguson KM, Abrams CS. Pleckstrin homology domains and the cytoskeleton. FEBS Lett. 2002; 513:71–76. [PubMed: 11911883]
41. Stephens LR, Jackson TR, Hawkins PT. Agonist-stimulated synthesis of phosphatidylinositol(3,4,5)-trisphosphate: a new intracellular signalling system? Biochim Biophys Acta. 1993; 1179:27–75. [PubMed: 8399352]
42. He J, Haney RM, Vora M, Verkhusha VV, Stahelin RV, Kutateladze TG. Molecular mechanism of membrane targeting by the GRP-1 PH domain. J Lipid Res. 2008; 49:1807–1815. [PubMed: 18469301]

NIH-PA Author Manuscript

NIH-PA Author Manuscript

NIH-PA Author Manuscript

43. Park WS, Heo WD, Whalen JH, O'Rourke NA, Bryan HM, Meyer T, Teruel MN. Comprehensive identification of PIP3-regulated PH domains from *C. elegans* to *H. sapiens* by model prediction and live imaging. Mol Cell. 2008; 30:381–392. [PubMed: 18471983]
44. Lemmon MA. Pleckstrin Homology (PH) domains and phosphoinositides. Biochem Soc Symp. 2007; 74:81–93. [PubMed: 17233582]
45. Rider MH, Bertrand L, Vertommen D, Michels PA, Rousseau GG, Hue L. 6-phosphofructo-2-kinase/fructose-2,6-bisphosphatase: head-to-head with a bifunctional enzyme that controls glycolysis. Biochem J. 2004; 381:561–579. [PubMed: 15170386]
46. Dumont JE, Dremier S, Pirson I, Maenhaut C. Cross signaling, cell specificity, and physiology. Am J Phys Cell Phys. 2002; 283:C2–C28.
47. Illies C, Gromada J, Fiume R, Leibiger B, Yu J, Juhl K, Yang SN, Barma DK, Falck JR, Saiardi A, et al. Inositol pyrophosphates determine exocytic capacity. Science. 2007; 318:1299–1302. [PubMed: 18033884]
48. Barker CJ, Wright J, Hughes PJ, Kirk CJ, Michell RH. Complex changes in cellular inositol phosphate complement accompany transit through the cell cycle. Biochem J. 2004; 380:465–473. [PubMed: 14992690]
49. Torres J, Domínguez S, Cerdá FM, Obal G, Mederos A, Irvine RF, Díaz A, Kremer C. Solution behaviour of myoinositol hexakisphosphate in the presence of multivalent cationsPrediction of a neutral pentamagnesium species under cytosolic/nuclear conditions. J Inorg Biochem. 2005; 99:828–840. [PubMed: 15708805]
50. Weiner OD, Neilsen PO, Prestwich GD, Kirschner MW, Cantley LC, Bourne HR. A PtdInsP(3)- and Rho GTPase-mediated positive feedback loop regulates neutrophil polarity. Nat Cell Biol. 2002; 4:509–513. [PubMed: 12080346]

NIH-PA Author Manuscript

NIH-PA Author Manuscript

NIH-PA Author Manuscript

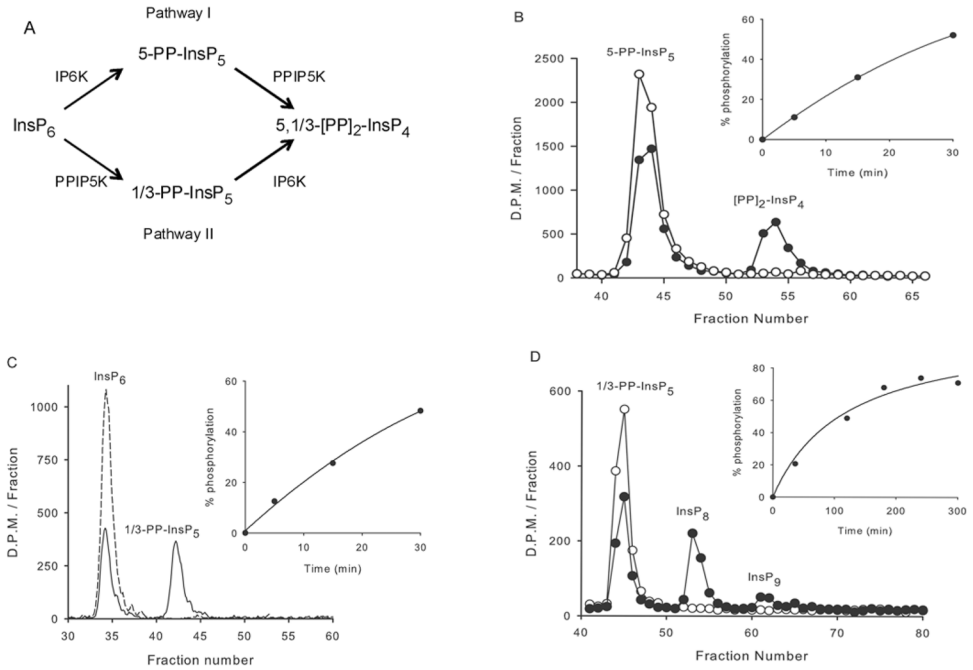

Figure 1. The contributions of PPIP5Ks to $[PP]_2$ -$InsP_4$ synthesis

(**A**) The two pathways of $[PP]_2$ -$InsP_4$ synthesis in mammalian cells. The structures of the diphosphoinositol polyphosphates are taken from information in [5,7,11]. The uncertainty concerning the precise placement of the 1/3-diphosphate group reflects an analytical impediment created by the axis of symmetry in the inositol ring. Thus 1-PP-$InsP_5$ and 3-PP-$InsP_5$ are an enantiomeric pair, and a stereoselective technique to distinguish between them has not yet been developed. This figure does not include the uncharacterized $InsP_8$ and $InsP_9$ observed in the present study, because of questions concerning their biological significance in mammalian cells (see the Results section). (**B**) A total of 0.2 ng of the PPIP5K1 kinase domain was incubated for either 0 min (open circles) or 15 min (filled circles) in 30 μl of kinase assay buffer, with approx. 5000 d.p.m. of 5-PP-[^{3}H]$InsP_5$. (**C**) In 30 μl of kinase assay buffer,17 ng of the kinase domain was incubated with approx. 0.035 μCi [^{3}H]$InsP_6$ for either 0 min (broken line) or for 20 min (solid line). (**D**) In 150 μl of kinase assay buffer, 500 ng of the kinase domain was incubated with approx. 1500 d.p.m. [^{3}H]$InsP_8$ for either 0 min (open circles) or 4 h (filled circles). All assays were acid quenched, neutralized and analysed by Partisphere SAX HPLC as described in the Materials and methods section, and radioactivity was assessed in either 1 ml fractions (**B** and **D**) or by using an in-line counter (**C**). The insets show the time course for each reaction. Recoveries of ^{3}H in all experiments were >85 % (see the Materials and methods section).

NIH-PA Author Manuscript

NIH-PA Author Manuscript

NIH-PA Author Manuscript

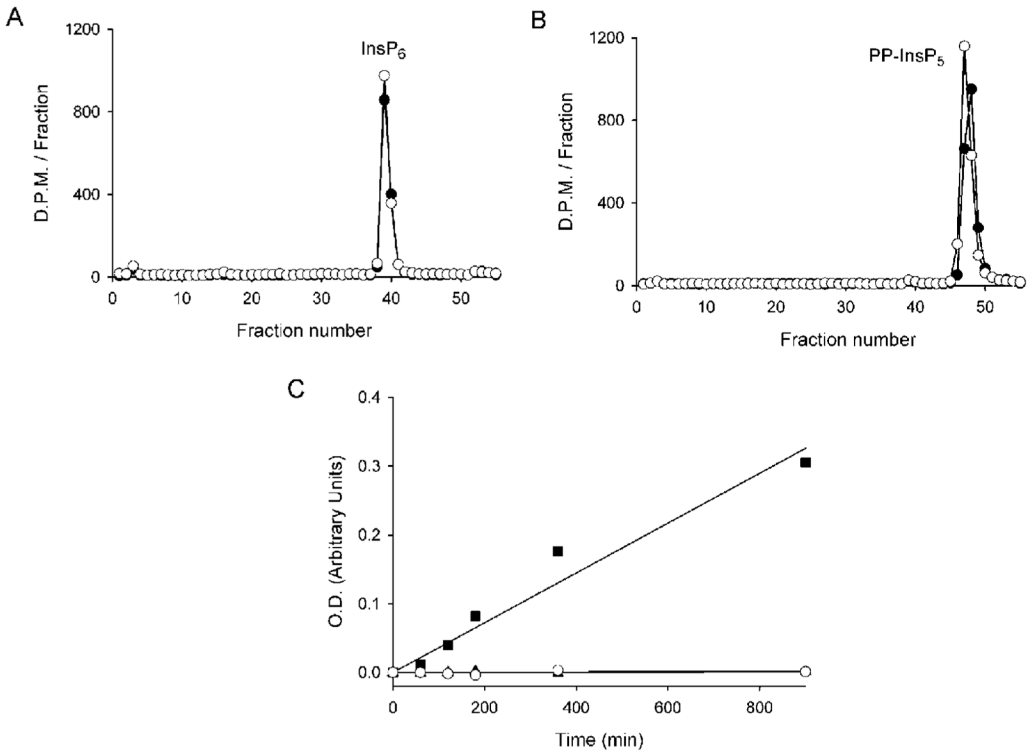

Figure 2. The phosphatase-like domains of PPIP5Ks do not have phosphatase activity

PBD1 (6 μg) was incubated with approx. 1500–2000 d.p.m. of either [^{3}H]InsP$_6$ (**A**) or 5-PP-[^{3}H]InsP$_5$ (**B**) in 120 μl of phosphatase assay buffer for 15 h at 37 °C (closed circles). Controls (open circles) did not contain enzyme. (**C**) 50 mM *p*-nitrophenyl phosphate replaced the inositol phosphates, and the assays contained 90 μg of either PBD1 (open circles) or PBD2 (closed triangles; these symbols are largely hidden by the open circles). Reactions were quenched with 1M NaOH and the A_{450} indicates the accumulation of *p*-nitrophenol. The closed squares represents the hydrolysis of *p*-nitrophenylphosphate by 90 ug of hMIPP. O.D., optical density (absorbance).

NIH-PA Author Manuscript

NIH-PA Author Manuscript

NIH-PA Author Manuscript

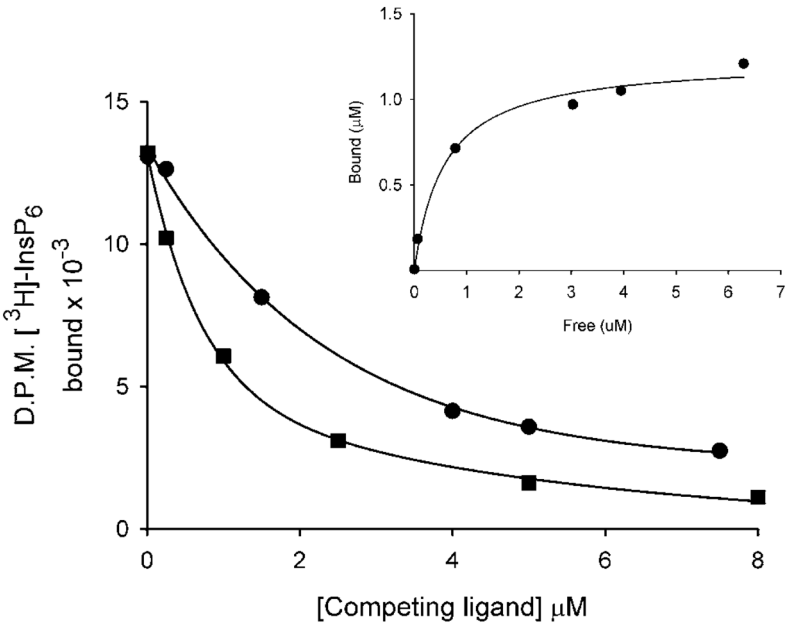

Figure 3. Use of a PEG precipitation assay to identify binding of $InsP_6$ and PtdIns(3,4,5)P_3 to PBD2

PBD2 (32 μg) was incubated with ^{3}H$InsP_6$ and increasing amounts of either non-radioactive $InsP_6$ (circles) or C_8 -PtdIns(3,4,5)P_3 (squares) as described in the Materials and methods section. Bound and free ligand was separated by a PEG precipitation technique (see Materials and methods section). The K_d for $InsP_6$ (0.57 μM) was calculated from the saturation binding plot (inset). The value of B_{max} was 0.6 mol/mol of protein.

NIH-PA Author Manuscript
NIH-PA Author Manuscript
NIH-PA Author Manuscript

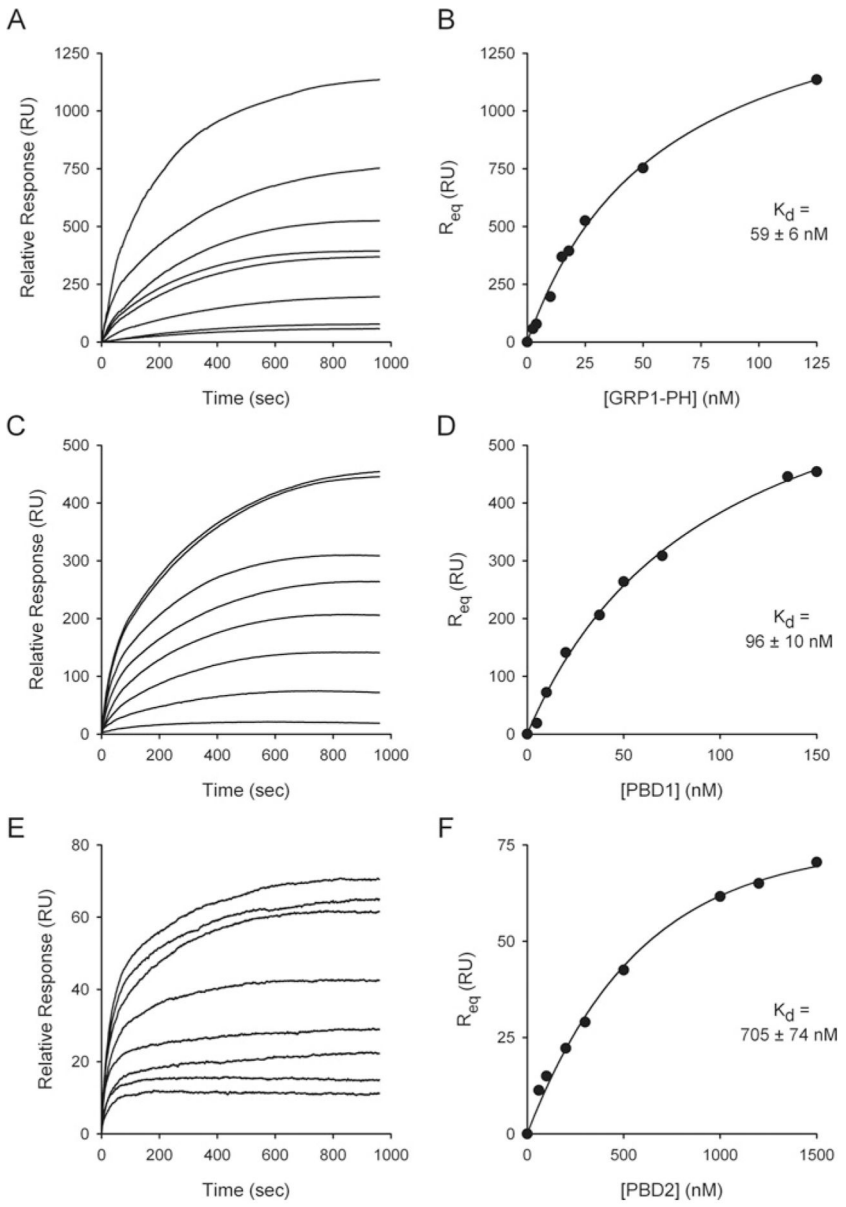

Figure 4. SPR-based equilibrium-binding analysis of the affinity for PtdIns(3,4,5)P_3 for the GRP1 PH domain, PBD1 and PBD2

Test protein was injected at 5 μl/min over immobilized PtdCho/PtdE/PtdIns(3,4,5)P_3 vesicles and the resulting changes in the RU are plotted as a function of time to yield the SPR binding sensorgrams. The resulting R_{eq} values are plotted as a function of the protein concentration, from which a K_d value was determined, as described in the Materials and methods section. (**A** and **B**) Data obtained from the GRP1 PH domain (2.5, 4, 10, 15, 18, 25, 50 and 125 nM). (**C** and **D**) Data obtained from PBD1 (5, 10, 20, 37.5, 50, 70, 135 and 150 nM). (**E** and **F**) Data obtained from PBD2 (60, 100, 200, 300, 500, 1000, 1200 and 1500 nM). S.E.M. of individual R_{eq} values are smaller than the symbols denoting the means.

NIH-PA Author Manuscript

NIH-PA Author Manuscript

NIH-PA Author Manuscript

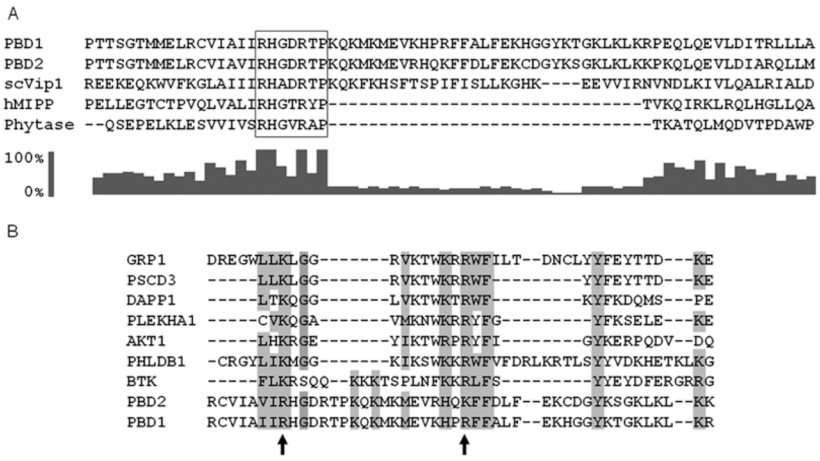

Figure 5. Evidence from multiple sequence alignments that PBD1 and PBD2 are unusual hybrid PtdIns(3,4,5)P_3-binding domains

(**A**) Previous molecular modelling studies [10] have identified residues 530–1047 as a phosphatase-like region of Vip1 from *Saccharomyces cerevisiae* (scVip); the N-terminus of this domain was aligned (using ClustalX) with corresponding residues in the PBDs of PPIP5K1 (residues 382–453), PPIP5K2 (residues 371–442), hMIPP and the *E. col.* phytase. The RHGXRXP acid-phosphatase motif in the PBDs is boxed. The bar graph (generated with ClustalX 2.0.10) shows the conservation score (on a scale of 0 to 100 %) for each residue in the alignment. (**B**) A separate ClustalX sequence alignment of PBD1, PBD2 and several PtdIns(3,4,5)P_3 -specific PH domains (GRP-1, PHLDB1 and PSCD3 are from mice; DAPP1, PLEKHA1, AKT1 and BTK are human sequences). The arrows mark two conserved basic residues in PBD1 (Arg^{399} and Arg^{417}) that were selected for mutagenesis studies. Other conserved amino acid residues that are identical or similar in nature have also been highlighted. GenBank® accession numbers: scVip1, NP_013514; hMIPP, AAH32504.1; Phytase, 9954897; PBD2, NP_056031.2; PBD1, AAH57395.1; GRP-1, AAB60876.1; PSCD3, EDL19040.1; DAPP1, AAH12924.1; PLEKHA1, AAH01136.1; AKT1, AAL55732.1; PHLDB1, AAH69853.1; BTK, NP_000052.1.

NIH-PA Author Manuscript

NIH-PA Author Manuscript

NIH-PA Author Manuscript

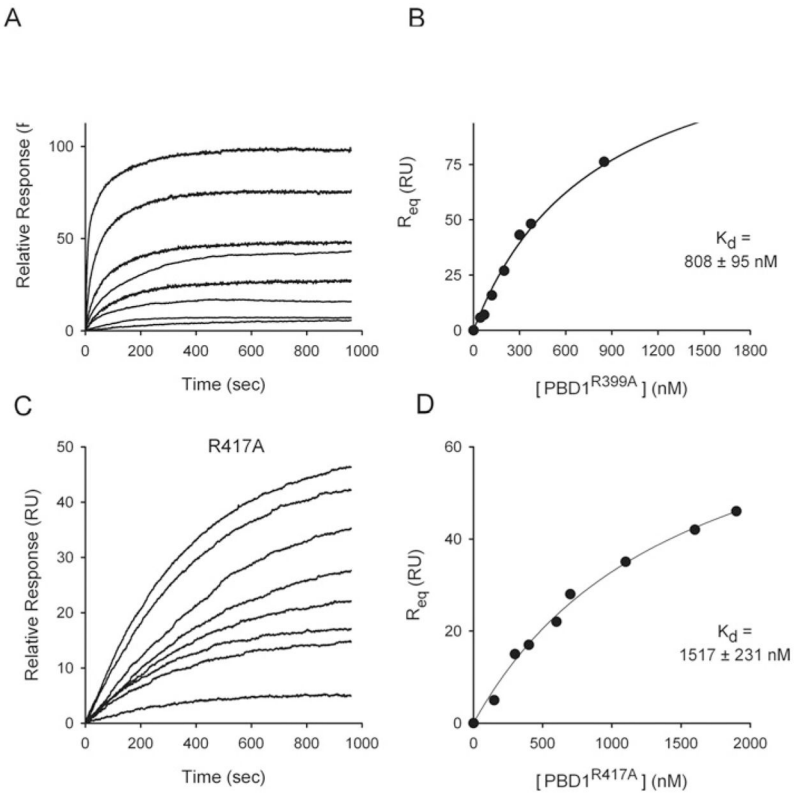

Figure 6. SPR-based equilibrium-binding analysis of the affinity for PtdIns(3,4,5)P_3 of two PBD1 mutants

Two arginine residues in PBD1 (that correspond with Arg^{399} and Arg^{417} in PPIP5K1) were mutated to alanine and the constructs R399A (at 45, 70, 120, 200, 300, 375, 850 and 1700 nM) (**A** and **B**) and R417A (at 150, 300, 400, 600, 700, 1100, 1600 and 1900 nM) (**C** and **D**) were injected at 5 μl/min over immobilized PtdCho/PtdE/PtdIns(3,4,5)P_3 vesicles and the resulting changes in the RU are plotted as a function of time to yield the SPR-binding sensorgrams (**A** and **C**), from which the K_d values were determined (**B** and **D**). The buffer contained 100 mM KCl, 6 mM $MgCl_2$, 5 mM Na_2 ATP and 25 mM Hepes (pH 7.2).

NIH-PA Author Manuscript
NIH-PA Author Manuscript
NIH-PA Author Manuscript

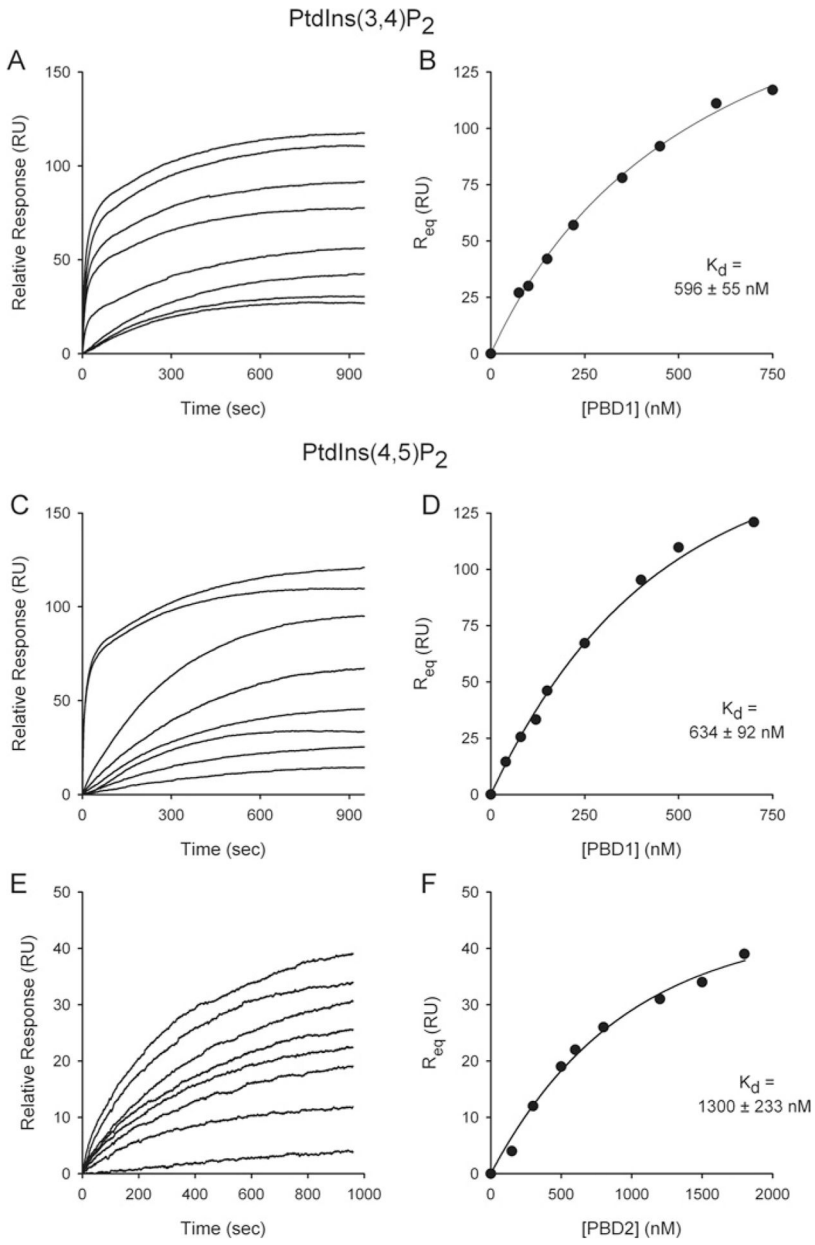

Figure 7. SPR-based equilibrium-binding analysis of the affinity for PtdIns(4,5)P_2 and PtdIns(4,5)P_2 for PBD1 and PBD2

Either PBD1 (**A**–**D**) or PBD2 (**E** and **F**) were injected at 5 μl/min over immobilized PtdCho/PtdE/PtdIns(3,4)P_2 vesicles (**A** and **B**) or PtdCho/PtdE/PtdIns(4,5)P_2 vesicles (**C**–**F**) and the resulting changes in the RU are plotted as a function of time to yield the SPR binding sensorgrams, from which the K_d values were determined. Peptide concentrations ranged from 75 to 1900 nM.

NIH-PA Author Manuscript

NIH-PA Author Manuscript

NIH-PA Author Manuscript

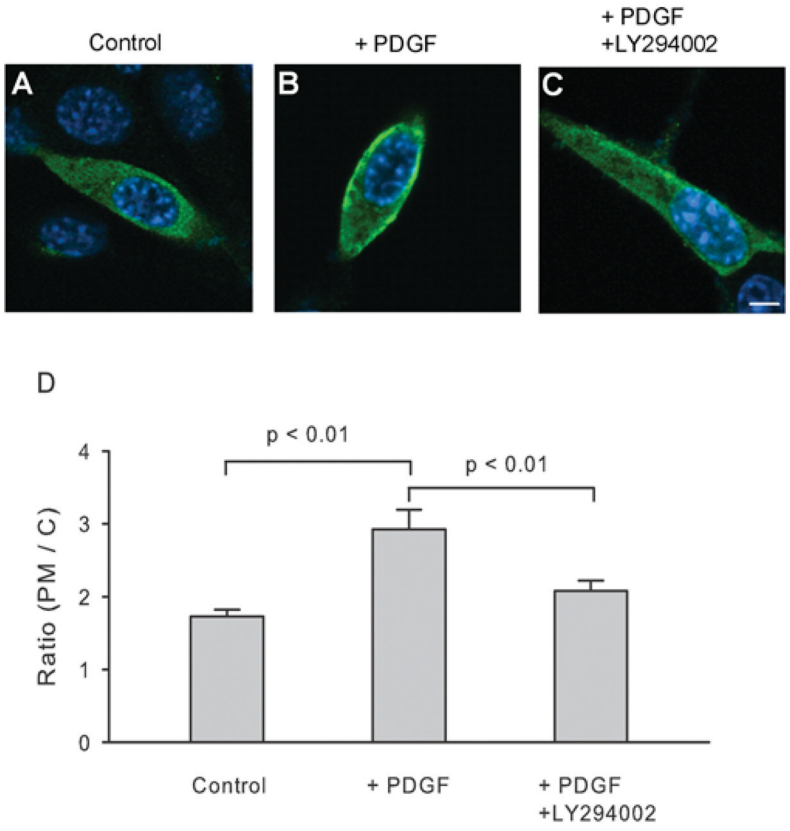

Figure 8. PDGF promotes translocation of PPIP5K to the plasma membrane in NIH 3T3 cells

At 1 day after transfecting NIH 3T3 cells with cDNA encoding FLAG-tagged PPIP5K1, the intracellular location of the enzyme was determined by confocal immunofluorescence microscopy. (**A**) Control. (**B**) Treatment with 50 ng/ml PDGF for 5 min. (**C**) 15 min pre-treatment with 100 μM LY294002 [50] before 50 ng/ml PDGF was added for 5 min. The scale bar represents 5 μm. (**D**) The concentration of PPIP5K at the plasma membrane (PM) is shown as a ratio to the concentration of kinase in the cytosol (C) [30]. Results are the means ± S.E.M. from 31–34 cells.

NIH-PA Author Manuscript

NIH-PA Author Manuscript

NIH-PA Author Manuscript

Table 1
Kinetic constants for PPIP5K1 catalytic domain

The k_{cat}/K_m ratios (specificity constants) were determined from the enzyme concentration and first-order rate constants for the metabolic reactions described in Figure 1, except for Ins(1,3,4,5,6)P_5 phosphorylation. The data for intracellular concentrations were taken from various sources. Several publications have put the cellular concentration of PP-InsP_5 in the 1–5 μM range (see [4] for a summary); a mid-range value of 2 μM is given in this Table. The values for the concentrations of Ins(1,3,4,5,6)P_5 and InsP_6 [48] are at the high end of a range of estimates [49]. MDD–HPLC analysis indicates that 1/3-PP-InsP_5 must be <10 % of the cellular concentration of 5-PP-InsP_5 [5,11].

Substrate	Concentration *in vivo* (M)	k_{cat}/K_m ($10^4 \times M^{-1}\ s^{-1}$)	[S]×k_{cat}/K_m (s^{-1})
5-PP-InsP_5	2×10^{-6}	384 ± 10	7.7
InsP_6	40×10^{-6}	4.8 ± 0.3	1.9
Ins(1,3,4,5,6)P_5	90×10^{-6}	0.3 ± 0.01	0.021
1/3-PP-InsP_5	0.2×10^{-6}	0.11 ± 0.04	0.0002